A Propagation Measurement Set-Up for MIMO System Channel Characterization and Preliminary Results

William J. Turney , Laddie T. Malek, Nicholas E. Buris

Motorola Labs, Motorola Inc.; 1301 East Algonquin Road Schaumburg, Il. 60196 room 2912 email: cwt001@email.mot.com; clm006@email.mot.com; nick.buris@motorola.com

Abstract

The correct performance assessment and characterization of Multiple Input Multiple Output (MIMO) systems requires the concurrent consideration of antennas and the propagation environment to a higher degree than ever before. In this paper we describe a measurement set-up and a measurement campaign aiming at the derivation of certain aspects of the propagation environment. In contrast to the majority of published methods, the described set-up is based on broadband sweeps using a Vector Network Analyzer (VNA) and long, low loss cables to enable magnitude and phase measurements. By construction, the in-home and outdoor–to-indoor environments are of primary focus for this paper. Preliminary measurements in an industrial office building confirm previously published cluster models and extend those to include non-horizontal plane directions of arrival and departure.

1. Introduction

In traditional Single Input Single Output (SISO) telecommunication system design, link budget calculations are based on using the maximum power gain of the transmit and receive antennas and without any polarization mismatch losses. Performance degradation due to antenna polarization efficiency and misalignment from the maximum gain orientation are understood and are quantified with studies such as [1]. In cases where the complexity of the environment deviates obviously from the simplest, Line of Sight (LOS) scenario, such as, for example, in measuring antennas at ground reflection ranges, the constructive and destructive interference of the LOS ray combining with a ground reflection are described via the antenna "height gain". MIMO systems try to judiciously exploit the environment and the presence of multipath to improve the link. Therefore, antenna design and propagation characteristics are intricately and inseparably related. Most of the literature has been devoted to propagation models for MIMO systems that are basically 2-dimensional. For example, TGn [2] describes various propagation environments in terms of clusters of rays with certain power and delay profiles that travel in the horizontal plane (i.e. zero elevation angle for Direction of Departure (DoD) and Direction of Arrival (DoA) for all the rays in the model). This paper describes a measurement effort to characterize the expected 3-dimensional nature of propagation indoor environments.

2. The Measurement System Set-Up

The block diagram for the data collecting system is shown in Figure 1. The basic system uses a 4-port VNA as a combined receiver transmitter. The system is currently designed to operate either near 2.4GHz or 5.7GHz. The receiving antenna is a narrow beam 24 inch, dual-polarized, parabolic dish with a 3dB beam width of approximately 12^0 at 2.4GHz and 5.5^0 at 5.7GHz. The height of the receiving antenna is 4.75 feet above the floor and is not easily adjustable. The antenna used for transmitting has a broad vertical beam and is approximately omni-directional in the azimuth plane. The transmit antenna can be either vertically or horizontally polarized. The height of this antenna is 5 feet for data shown in this paper, but can be adjusted over a range of approximately 5-20 feet. Low loss, phase-stable coaxial cables are used to connect the various components of the system. Cable lengths limit antenna separation to approximately 150 feet. Band change is accomplished by changing all antennas and filters that comprise the system. The system is very similar to the system used by others [3,4] with the additional capability of capturing data at different elevation angles.

In operation, the elevation angle of the parabolic antenna is manually adjusted to the desired angle. A range of elevation angles from -12^0 to 84^0 degrees in increments of 12^0 was used. The azimuth positioner automatically moves the parabolic antenna to a new position when commanded by the control system. Data was collected over an azimuth angle range of 360^0 at 160 positions for each elevation angle setting. At each azimuth position the

positioner was halted, and a chirp signal of 500-MHz bandwidth was transmitted in the frequency range of either 2.25-2.75 GHz or 5.35-5.85GHz. Complex frequency domain data was collected at 401 points over the 500-MHz bandwidth. By using a multiport VNA and a dual polarized receiving antenna, co-polarization and cross polarization data was collected simultaneously.

3. Preliminary Results

The measurement set-up described above has been used to obtain results inside a large commercial building in Schaumburg, IL. The building, a two story facility, consists of long hallways with electronics laboratories and large office spaces on either side. Measurements were performed at the second floor. There are a lot of metal pipes hidden above a dropped ceiling and the floor is raised with tile to cover a lot of fiber cables and other infrastructure. The layout is depicted in Figure 2.

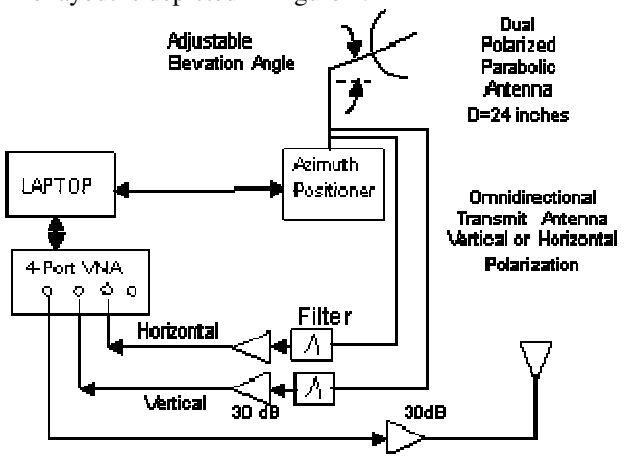

Figure 1: Data Collection System

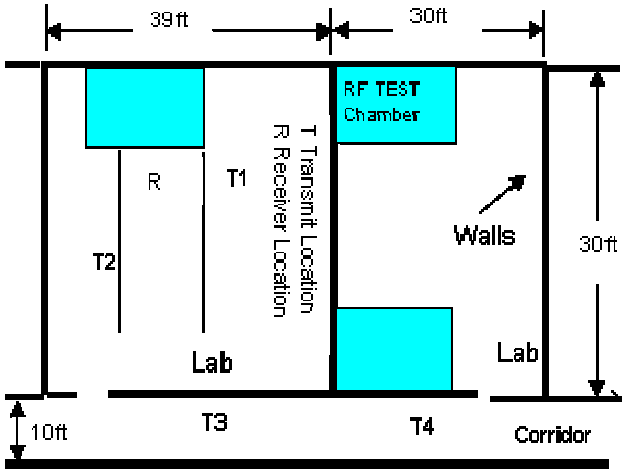

Figure 2: Building Layout

3.1 Elevation Angle of Arrival

Data was collected at both frequency bands with the antennas placed at four different locations in the environment described above. For two of the locations, both antennas were within the same room separated 16 to 20 feet. Both of these locations represent an Obstructed-Line-Of-Sight (OLOS) environment. For the other two locations, one of the antennas was in the corridor and the other antenna was in the laboratory. The wall between the laboratory and the corridor is constructed of plaster covered concrete blocks and has high RF penetration loss. Transmitter (T) and receiver (R) locations are marked in Figure 2 and were interchanged during the measurement campaign for the corridor-to-room measurements.

Measured data was preprocessed by using special calibration data to remove the gains and frequency dependencies of the amplifiers, coaxial cables, and filters in the system. The antenna frequency dependency and the effects of antenna sidelobes were not removed for the data shown in this paper. For each elevation angle that data was gathered, processing of the data consisted of calculating the average received power over the 500-MHz bandwidth and taking the Inverse Discrete Fourier Transform (IDFT)of the complex data. This was done for each of the 160 points that comprise a full rotation of the dish antenna.

Time-space data plots are shown in Figure 3 for several different elevation angles at location T3. The data shown was measured in the 2GHz band, but are representative of all locations measured for both the 2 and 5GHz bands. Absolute delay in nanoseconds is given by the vertical axis and azimuth in degrees is given by the horizontal axis. The relative intensity of the signal (in dB) over space-time is depicted by color. The data shown in each plot consists of data normalized to the largest signal value at the particular elevation angle of the measurement. This technique has been used by others [3,5,6] and permits easy cluster identification and cluster parameter extraction. As can be seen, the cluster structure is not a strong function of elevation (especially the strongest cluster located near

an azimuth location of 210^0). This fact has been noted by others [3] and has been incorporated into the TGn propagation model [2] and the WINNER propagation models [7]. The number of clusters, angular spread and RMS time delay for the environment measured fall within the guidelines of the TGn model for this type of environment.

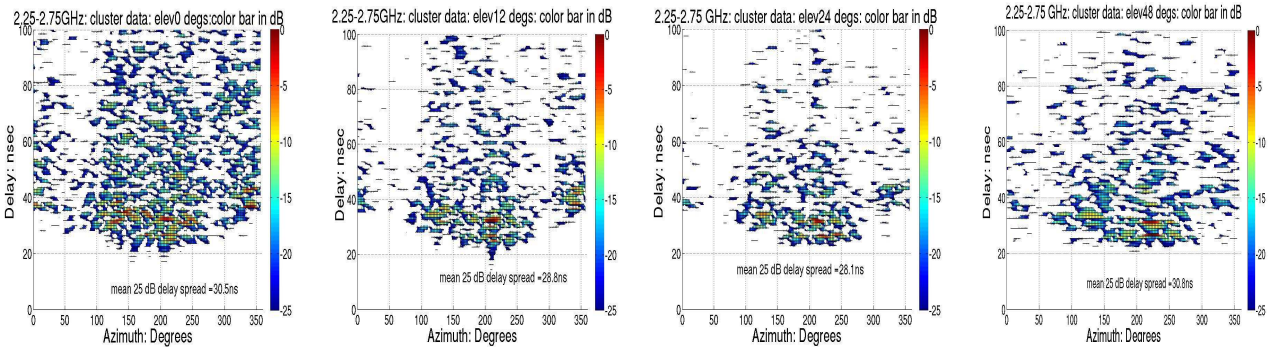

Elevation=0 degrees | Elevation=12 degrees | Elevation=24 degrees | Elevation=48 degrees

Figure 3: Space-Time Plots

However, there is a signal power, elevation angle dependency that has not been emphasized enough in published models. If the un-normalized average received power over the measured signal bandwidth (500 MHz) is plotted at each azimuth location as shown in Figure 4, it is clear that the power is the largest at the azimuth location of the clusters. Thus selecting the azimuth of a cluster and keeping it fixed (ϕ=210^0 here), Figure 5 depicts the power variation versus elevation angle. Although Figure 5 is for ϕ=210^0, the range of power variation over elevation was approximately the same for all locations measured and for both frequency bands. Additionally, similar behavior was shown for the cross polarization component.

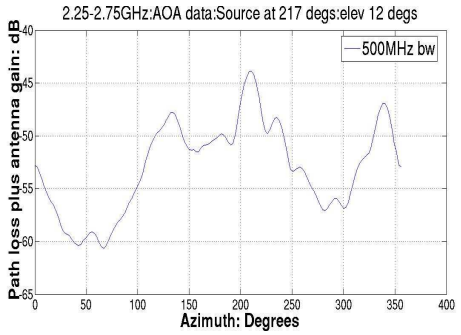

Figure 4: Power vs. Azimuth

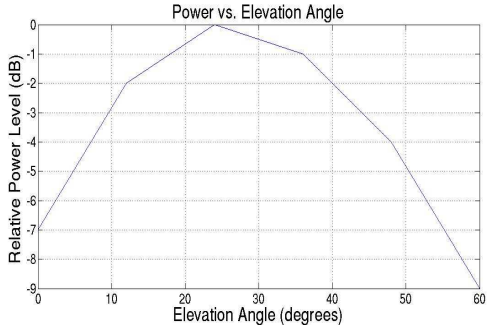

Figure 5: Relative power vs. Elevation

3.2 Cross Polarization Characteristics

The data has also been post processed to determine the polarization conversion factor, $c = E_{cop} / E_{xpol}$.

Consider a single ray departing the transmitter and arriving at the receiver (observation point). Approximately, the polarization conversion factor for that ray can be expressed in terms of a ratio of products describing the various reflections. With many rays vectorially combining at the observation point, the polarization conversion factor should be of the form:

$$c = \frac{\sum_{all\ rays} \Gamma_{\perp a}\Gamma_{\perp b}\cdots\Gamma_{\perp n}}{\sum_{all\ rays} \Gamma_{//a}\Gamma_{//b}\cdots\Gamma_{//n}} \approx \left.\frac{\Gamma_{\perp a}\Gamma_{\perp b}\cdots\Gamma_{\perp n}}{\Gamma_{//a}\Gamma_{//b}\cdots\Gamma_{//n}}\right|_{do\ \min\ ant\ ray} \qquad \text{Eq.(1)}$$

Where the Γ's indicate some effective reflection coefficient for each polarization on the reflecting surfaces of the environment. For the purposes of this argument, these Γ's include the effects of diffraction and the polarization

rotation/conversion imposed on each ray from mere geometric circumstances. The approximation simply equates the polarization conversion factor to just that of the dominant ray (i.e. it assumes that the power of the dominant ray is much larger than that of the sum of all other rays). Expressing this in dB, results in a sum (and difference) of random variables which should follow the central limit theorem and have a lognormal distribution. Indeed, Figure 6 below shows that this is approximately true. Additionally the mean of the distribution is 2.5 dB which is close to suggested XPR for use in the TGn models and that observed by others [2,8,9] Even though the central limit theorem is actually observed by adding just a few random variables together [10,11], the deviations from lognormal are attributed to the approximation made in Eq.(1).

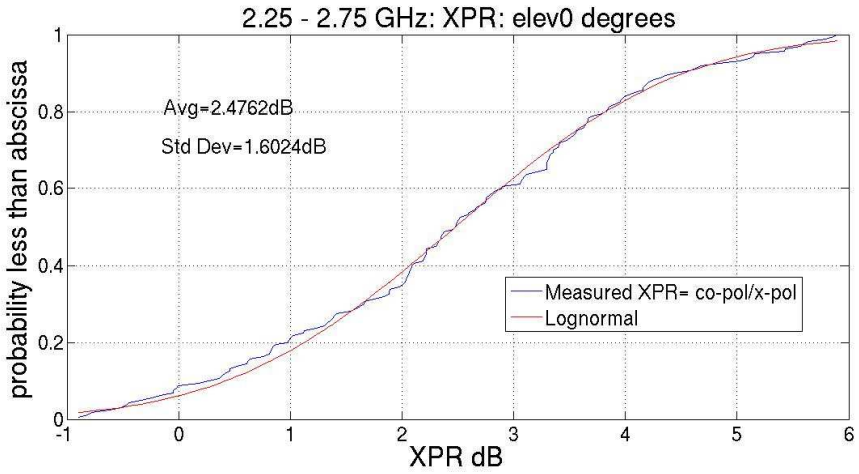

Figure 6: Cumulative Distribution Function of Cross Polarization Ratio

4. Conclusions

Measurements in a commercial building indicate that the AOA in elevation for an indoor environment is elevated above the horizon for systems operating in 2-6 GHz frequency range. This constitutes one of the steps in the construction of a 3-D model. The measurement campaign will be extended to include residential housing. Additionally, the cross polarization ratio was found to have an approximate lognormal distribution. This can be used to extend statistical modeling capabilities for system that utilize orthogonal polarization.

5. References

1. D.C. Cox, et al., "Cross-Polarization Coupling Measured for 800MHz Radio Transmission In and Around Houses and Large Buildings", IEEE Trans. Antennas Propagation, vol. AP-34, No.1, pp. 83-87, January 1986.
2. IEEE P802.11, "TGn Channel Models", May 10, 2004.
3. Spencer, Jeffs, Jensen, and Swindlehurst, "Modeling the Statistical Time and Angle of Arrival Characteristics of an indoor Multipath Channel", IEEE Journal on Selected Areas in Communication, Vol.18, No.3, March 2000.
4. Boonvisat, et al, "Indoor Propagation Channel Measurement of Ultra Wideband Antenna with Robotic" Proc. ISCIT, 2005.
5. Yu,Li, and Ho, "Measurement Investigation of Tap and Cluster Angular Spreads at 5.2GHz", IEEE Transaction on Antennas and Propagation, Vol. 53, No. 7, 2005.
6. Chong, Laurenson, and McLaughlin, "Statistical Characterization of the 5.2GHz Wideband Directional Indoor Propagation Channels with Clustering and Correlation Properties", IEEE VTC 2002 Proceedings.
7. IST-4-027756 WINNER II Channel Models, parts I and II, September 30, 2007.
8. Kyritsi, Cox, "Propagation Characteristics of Horizontally and Vertically Polarized Electric Fields in an Indoor Environment: Simple Model and Results", IEEE VTC Fall 2001.
9. Shafi, Zhang, Moustakas, Smith, Molisch, Tufvesson, Simon, " Polarized MIMO Channels in 3-D: Models, Measurements and Mutual Information", IEEE Journal on Selected Areas in Communications, Vol. 24, No. 3, March 2006.
10. A. Papoulis, "Probability, Random Variables and Stochastic Processes", section 8-6, Mac Graw-Hill, 1965.
11. G. Hess, "Land-Mobile Radio System Engineering", Artech House, pp. 49-51, 1993.